

Mass spectrometry



High precision *in situ* Rb-Sr age dating

Authors

A. Cruz-Uribe
University of Maine,
Orono, Maine, USA

D. Bevan
University of Bristol,
Bristol, UK

G. Craig, J. Roberts, C. Bouman,
N. Lloyd, J. Schwieters

Thermo Fisher Scientific,
Bremen, Germany

Keywords

Neoma MS/MS MC-ICP-MS,
Collision/Reaction Cell, Pre-cell Mass
Filter, Rubidium-Strontium age dating

Goal

To demonstrate how the Thermo Scientific™ Neoma™ MS/MS MC-ICP-MS can be used for *in situ* Rb-Sr age dating.

Introduction

Radiometric dating of geological materials using the ^{87}Rb – ^{87}Sr beta decay system is a well-established geochronological technique which has been exploited for over 80 years. By its nature, beta decay produces a daughter nuclide that isobarically interferes with its parent during mass-spectrometric analysis. To resolve ^{87}Rb from ^{87}Sr , a mass resolving power of $M/\Delta M \sim 300,000$ is required. Such a high mass resolving power is not typically achievable by high precision isotope ratio mass spectrometers.

The development and coupling of collision/reaction cells (CRC) to inductively-coupled plasma mass spectrometers permits *in situ* radiogenic Sr isotopic analysis of high Rb/Sr minerals by using a suitable reaction gas within a collision cell¹ to react with the Sr⁺ ions but not the interfering Rb⁺ ions (Figure 1)^{2,3}. Such an approach has been successful in laser ablation Rb–Sr dating using single collector inductively coupled plasma mass spectrometers equipped with CRCs and pre-cell quadrupole mass filters (ICP-TQ-MS)^{4–6}.

Analytical precision is an important limit in such work, and as a result, many of the previous studies have focused on samples containing minerals with very high Rb/Sr (e.g. $^{87}\text{Rb}/^{86}\text{Sr}$ ratios >500) or samples that are particularly old (>1 Ga). Here, we demonstrate the potential of the Neoma MS/MS MC-ICP-MS, a collision cell MC-ICP-MS with a magnetic sector pre-cell mass filter, for high precision *in situ* Rb-Sr dating of a wider range of geological targets.

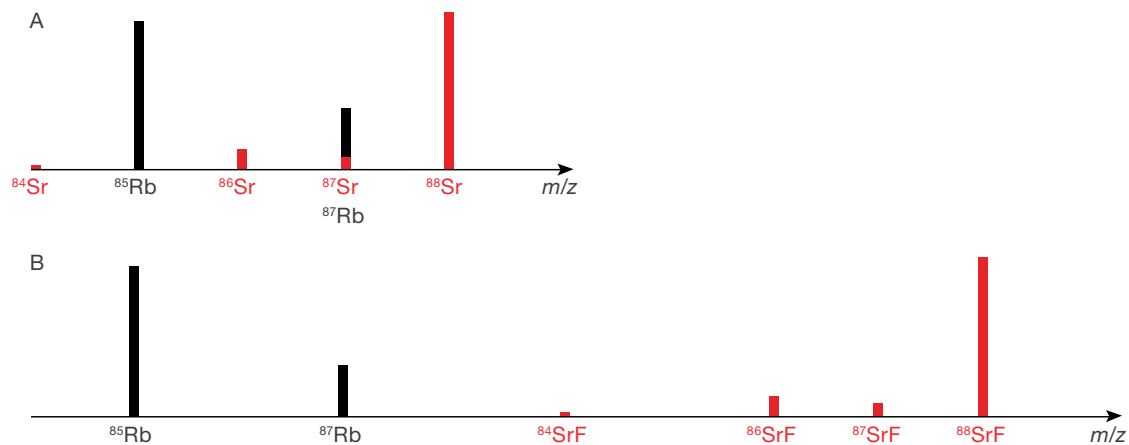


Figure 1. Schematic showing how CRC technology can be used to separate out the isobaric interferences (^{87}Rb , ^{87}Sr). (A) Without CRC – no separation of ^{87}Rb and ^{87}Sr , (B) Using SF_6 as a reaction gas creates a mass separation between Rb and Sr.

Methods

Neoma MS/MS MC-ICP-MS

Neoma MS/MS MC-ICP-MS^{7,8} uses the same principle of filter, react and separate pioneered with triple quadrupole ICP-MS (ICP-TQ-MS) (Figure 2). However, the Neoma MS/MS MC-ICP-MS offers the additional benefit of simultaneous isotope analysis, allowing for ultimate isotope ratio precision and accuracy.

Neoma MS/MS MC-ICP-MS comprises three main components; (i) the pre-cell mass filter, (ii) the hexapole CRC, and (iii) the magnetic sector (Figure 2).

The pre-cell mass filter allows effective removal of the sample matrix, preventing the creation of molecular interferences inside the CRC and cleaning up the mass spectra so that the analyte can be detected interference-free.

Unlike ICP-TQ-MS, the pre-cell mass filter in the Neoma MS/MS MC-ICP-MS is based on magnetic sector technology. It therefore does not compromise on sensitivity and produces predictable exponential mass bias for accurate internal normalization⁷.

The hexapole CRC can be pressurized with reactive gases to selectively generate reaction products thereby effectively removing isobaric interferences. The magnetic sector of Neoma MS/MS MC-ICP-MS separates out the isotopes of interest. The enhanced variable multicollector detector array with 11 Faraday cup detectors maximizes sample usage and enables ultimate precision through the simultaneous measurement of all isotopes of interest, allowing simultaneous measurement of Rb and SrF in one line (Table 1).

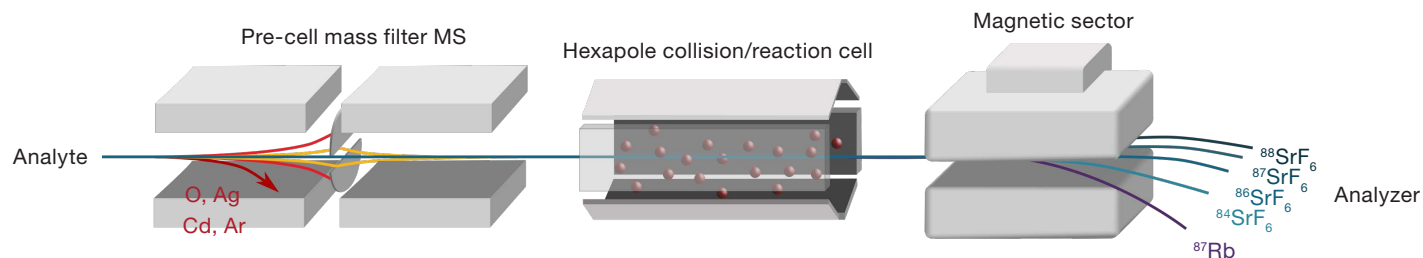


Figure 2. Schematic of key technological components of Neoma MS/MS MC-ICP-MS

Table 1. Cup Configuration

Cup	L5	L4	L3	L2	L1	C	H1	H2	H3	H4	H5
Rb/Sr	^{85}Rb	^{87}Rb	^{88}Sr	–	–	–	–	^{84}SrF	^{86}SrF	^{87}SrF	^{88}SrF
Amplifier	$10^{11}\Omega$	$10^{11}\Omega$	$10^{11}\Omega$	–	–	–	–	$10^{13}\Omega$	$10^{13}\Omega$	$10^{13}\Omega$	$10^{11}\Omega$

The Neoma MS/MS MC-ICP-MS was equipped with the Jet Interface using the high sensitivity X-skimmer and Jet-sampler cones. The Neoma MS/MS MC-ICP-MS set-up conditions are shown in Table 2. The Neoma MS/MS MC-ICP-MS tune parameters were set to achieve the highest sensitivity.

Table 2. Neoma MS/MS setup conditions

Parameter	Value
RF power [W]	1300
Cool gas [L min ⁻¹]	14
Aux gas [L min ⁻¹]	0.8
Neb gas [L min ⁻¹]	0.98
Wien filter electric field [V]	320
Wien magnetic field [%]	50
Wien center mass	⁸⁶ Sr
Pre-filter slit position [%]	60
CCT entry [V]	-45
CCT bias [V]	0
RF amplitude [%]	100
CCT exit 1 [V]	-85
CCT exit 2 [V]	-100
CCT SF ₆ [mL min ⁻¹]	0.075

In these experiments, sample was introduced to the Neoma MS/MS MC-ICP-MS via an Elemental Scientific Lasers™ (ESL) imageGEO193™ laser ablation system equipped with an ESL TwoVol3 ablation cell. The laser set-up conditions are shown in Table 3.

Table 3. ESL imageGEO193 setup conditions

Parameter	Value
Fluence [J cm ⁻²]	3.5
Spot size [μm]	50 or 100
Spot shape	circle
Repetition rate [Hz]	12
Dwell time [s]	40
He [L min ⁻¹]	1.00
N ₂ [mL min ⁻¹]	3.00

Laser parameters were controlled via the ESL NWR Laser plugin supplied within the Thermo Scientific™ Qtegra™ Intelligent Scientific Data Solution™ (ISDS) Software in Neoma MS/MS. This allows bi-directional communication between the two platforms, useful for sharing sample lists, triggering, and data processing. Similar plugins for Qtegra ISDS are available for other laser ablation systems.

Time resolved analyses were processed using a Rb-Sr data reduction scheme (DRS) in Lolite 4⁹.

The pre-cell mass filter was configured to filter the mass range around Sr and Rb (78-94 amu) to remove matrix elements that might otherwise isobarically interfere with the reaction product SrF (e.g. ¹⁰³Rh and ¹⁰⁷Ag; Figure 3a). By cleaning up the mass spectra, the pre-cell mass filter allows us to be confident that only the reactant (SrF) is being analyzed (Figure 3b).

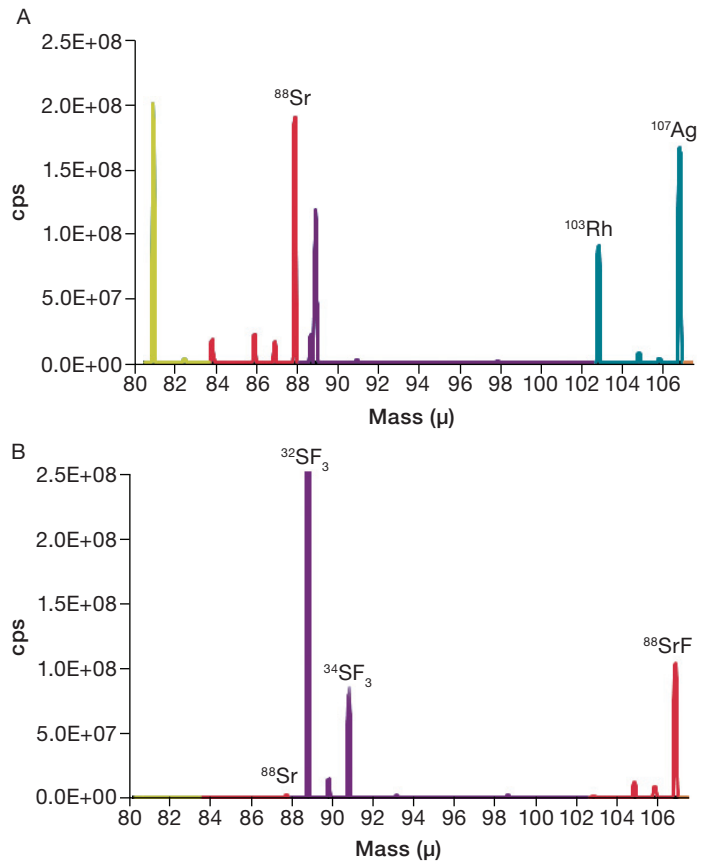


Figure 3. Pre-cell mass filter provides a clean spectra for reaction products for *in situ* Rb-Sr dating. (A) Without pre-cell mass filtering, a number of interferences are observed in the mass range for SrF ($m/z = 103-107$). (B) By applying a narrow filter window, matrix elements are removed such that SrF is the only observable mass in the mass range 103-107.

Samples

A number of different samples were measured to demonstrate the capabilities of Neoma MS/MS MC-ICP-MS for Rb/Sr dating:

1. NIST®, MPI-DING and USGS reference glasses,
2. Plagioclase feldspars from the Shap and Dartmoor granite intrusions,
3. Biotite from garnet-bearing schist Ra-D72 from the Mooselookmeguntic contact aureole, western Maine, USA

Results

Reference glasses

Six reference glasses were measured for the $^{87}\text{Sr}/^{86}\text{Sr}$ and $^{87}\text{Rb}/^{86}\text{Sr}$ ratio. To minimize the effects of matrix mismatch, the samples were normalized against materials of a similar composition (Table 4). Samples were also corrected for mass bias using the $^{88}\text{Sr}/^{86}\text{Sr}$ ratio.

Table 4. Summary of reference glasses analyzed and the primary standard used for normalization

Sample	Type	Primary reference material
NIST SRM612	Silicate glass	NIST SRM 610
MPI-DING StHs6/80-G	Andesite glass	MPI-DING T1-G
USGS BCR-2G	Basalt glass	MPI-DING KL2-G
USGS BHVO-2G	Basalt glass	MPI-DING KL2-G
MPI-DING ML3B-G	Basalt glass	MPI-DING KL2-G
MPI-DING GOR132-G	Komatiite glass	MPI-DING GOR128-G

The results are shown in Table 5 and Figure 4. The external precision (2 RSD, $n=10$) of the $^{87}\text{Sr}/^{86}\text{Sr}$ ratios is less than 1‰ for all samples, except for NIST SRM612 and MPI-DING GOR132-G which have low Sr concentrations, 70 ppm and 15 ppm respectively. This external precision of the $^{87}\text{Sr}/^{86}\text{Sr}$ ratios approach the theoretical limits of precision dictated by counting statistics (Figure 5). Note that the use of $10^{13}\ \Omega$ amplifiers in this case means that Johnson-Nyquist noise is not the dominant factor in the total measurement uncertainty. The use of longer ablation dwell times could be used to further decrease the analytical uncertainty.

The measured $^{87}\text{Sr}/^{86}\text{Sr}$ ratios are accurate within 0.7‰ of the reference $^{87}\text{Sr}/^{86}\text{Sr}$ ratios (Figure 4B). This level of accuracy is sufficient for most applications as natural variations in $^{87}\text{Sr}/^{86}\text{Sr}$ span a large range.

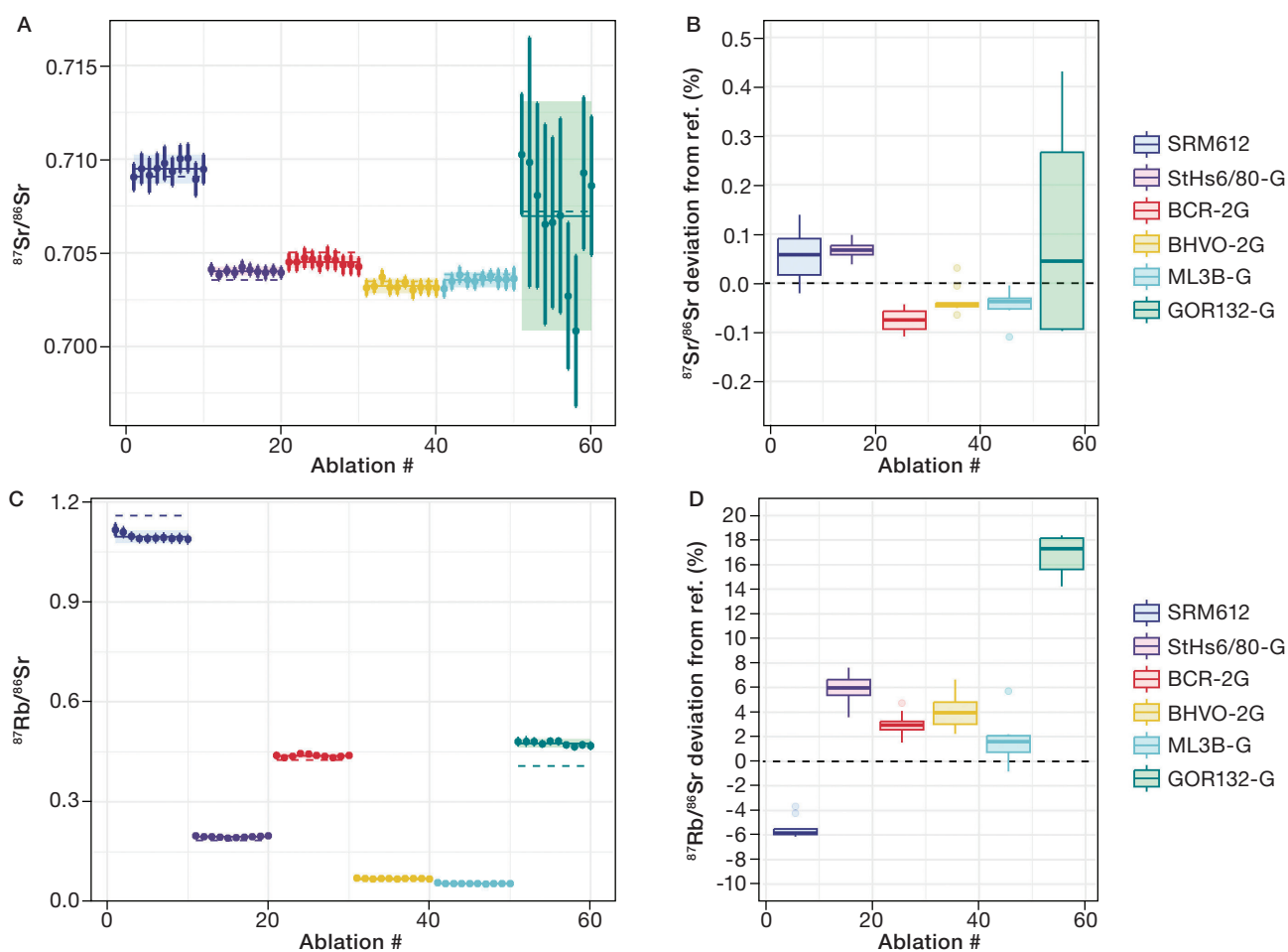


Figure 4. Summary of reference glass $^{87}\text{Sr}/^{86}\text{Sr}$ and $^{87}\text{Rb}/^{86}\text{Sr}$ analysis. (A) $^{87}\text{Sr}/^{86}\text{Sr}$ for the six reference glasses. Error bars given are 2 SE. Horizontal lines show average and 2 SD of 10 replicate analyses. Dashed lines show the reference value. (B) $^{87}\text{Sr}/^{86}\text{Sr}$ deviation from reference value as a percentage. (C) $^{87}\text{Rb}/^{86}\text{Sr}$ for the six reference glasses. (D) $^{87}\text{Rb}/^{86}\text{Sr}$ deviation from reference value as a percentage.

Table 5. Summary of reference glass $^{87}\text{Sr}/^{86}\text{Sr}$ and $^{87}\text{Rb}/^{86}\text{Sr}$ analysis. The reference $^{87}\text{Sr}/^{86}\text{Sr}$ values are shown for comparison. In the absence of reference $^{87}\text{Rb}/^{86}\text{Sr}$ values for the glasses, calculated $^{87}\text{Rb}/^{86}\text{Sr}$ values were determined using atomic weights, the measured $^{87}\text{Sr}/^{86}\text{Sr}$ composition, the concentrations of Rb and Sr and natural isotopic abundances.

	n	Rb (ppm)	Sr (ppm)	$^{84}\text{Sr}/^{86}\text{Sr}$	2 SD	2 RSD (%)	$^{87}\text{Sr}/^{86}\text{Sr}$	2 SD	2 RSD (%)	Ref. $^{87}\text{Sr}/^{86}\text{Sr}$	$^{87}\text{Rb}/^{86}\text{Sr}$	2 SD	2 RSD (%)	Calc. $^{87}\text{Rb}/^{86}\text{Sr}$
SRM612	10	29.7	70.4	0.0560	0.0002	0.4	0.7095	0.0008	0.11	0.70906	1.095	0.019	1.8	1.1587
StHs6/80-G	10	28.8	483.3	0.0551	0.0002	0.3	0.7040	0.0002	0.03	0.70354	0.195	0.005	2.4	0.1842
BCR-2G	10	44.8	296.8	0.0547	0.0003	0.6	0.7045	0.0003	0.05	0.70503	0.438	0.008	1.9	0.4252
BHVO-2G	10	1.6	421.9	0.0548	0.0003	0.5	0.7032	0.0004	0.06	0.70347	0.070	0.002	2.5	0.0672
ML3B-G	10	5.7	299.2	0.0558	0.0003	0.5	0.7036	0.0004	0.06	0.70385	0.055	0.002	3.5	0.0541
GOR132-G	10	2.2	15.0	0.0611	0.0082	13.5	0.7070	0.0061	0.87	0.70720	0.475	0.013	2.7	0.4069

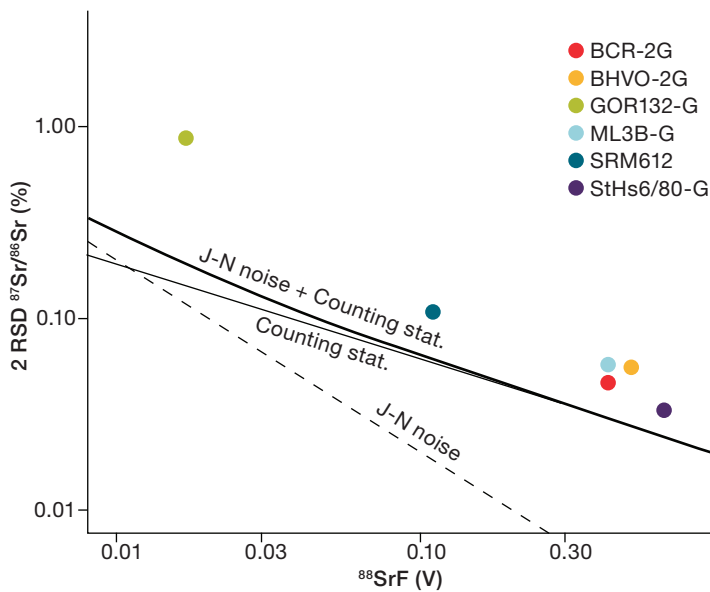


Figure 5. Comparison between external precision on $^{87}\text{Sr}/^{86}\text{Sr}$ of reference glasses with theoretical limit from Johnson noise and counting statistics

For the $^{87}\text{Rb}/^{86}\text{Sr}$ ratio, the external precision is less than 4% in all samples (Table 5). The measured $^{87}\text{Rb}/^{86}\text{Sr}$ ratios are accurate within 6% of the calculated $^{87}\text{Rb}/^{86}\text{Sr}$ ratio, with the exception of MPI-DING GOR132-G which had a very low Rb concentration of 2 ppm (Figure 4D).

Table 6. Comparison between Neoma MS/MS MC-ICP-MS and single collector triple quadrupole for USGS BCR-2G.

Sample	Instrument	n	Rb (ppm)	Sr (ppm)	$^{87}\text{Sr}/^{86}\text{Sr}$	2SD	2RSD (%)	Accuracy (%)	$^{87}\text{Rb}/^{86}\text{Sr}$	2SD	2RSD (%)	Accuracy (%)
USGS BCR-2G	Neoma MS/MS	10	44.8	296.8	0.7045	0.0003	0.05	-0.07	0.438	0.008	1.9	3.0
USGS BCR-2G	ICP-TQ-MS	18	47.0	326.0	0.7048	0.0048	0.68	-0.03	0.404	0.008	1.9	-5.1

We can make a rough comparison of the multicollector MS/MS approach and single collector triple quadrupole¹⁰ by looking at $^{87}\text{Rb}/^{86}\text{Sr}$ and $^{87}\text{Sr}/^{86}\text{Sr}$ ratios obtained on USGS BCR-2G using similar laser conditions (Table 6). The precision of the $^{87}\text{Sr}/^{86}\text{Sr}$ ratios collected with the Neoma MS/MS MC-ICP-MS are at least an order of magnitude better than using an ICP-TQ-MS. This is due to the precision of the $^{87}\text{Sr}/^{86}\text{Sr}$ ratio achievable being primarily governed by counting statistics. Therefore, the high sensitivity, high ion extraction of Neoma MS/MS MC-ICP-MS, coupled with static multicollection, means that a lower $^{87}\text{Sr}/^{86}\text{Sr}$ precision is easily obtainable. By comparison, the precision of the $^{87}\text{Rb}/^{86}\text{Sr}$ ratio is largely controlled by downhole fractionation of the Rb/Sr ratio during laser ablation. Therefore, similar precisions of the $^{87}\text{Rb}/^{86}\text{Sr}$ ratio are obtainable by Neoma MS/MS MC-ICP-MS and the single collector triple quadrupole¹⁰ (Table 6). The accuracy of the $^{87}\text{Sr}/^{86}\text{Sr}$ and $^{87}\text{Rb}/^{86}\text{Sr}$ are the same for both systems suggesting equally effective removal of matrix interferences for both systems.

Plagioclase and K-feldspar in granite

Two granite samples obtained from the University of Bristol, Shap Granite (SG-3) and Dartmoor Granite (DG-4), were measured. Other samples from the same locations (SG-1 and DG-1), had previously been measured on the prototype Thermo Scientific™ Proteus™ and Vienna MC-ICP-MS/MS, as well as the Thermo Scientific™ iCAP™ TQ ICP-MS^{7,11}.

Results from the two samples were normalized to the reference glass NIST SRM610¹². As SRM610 has a very different matrix to the granite samples, a glass/feldspar correction factor was applied to the $^{87}\text{Rb}/^{86}\text{Sr}$ ratios. We adopt the approach of Bevan et al.¹¹ of measuring isochrons in materials of known and similar mineralogy (in this case SG-3) to apply a correction factor (1.200) on the $^{87}\text{Rb}/^{86}\text{Sr}$ ratio of DG-4.

Our analysis of 43 ablation spots of plagioclase and K-feldspar in DG-4 had a calculated date of 283.54 ± 1.64 Ma (2σ , Figure 6). *In situ* Rb/Sr analysis of the related sample DG-1 with the single collector iCAP TQ ICP-MS⁷ gave a calculated Rb/Sr date of 284.6 ± 14.7 Ma (2σ , Figure 6)¹¹.

The 100-fold increase in sensitivity of Neoma MS/MS ICP-MS relative to the iCAP TQ ICP-MS results in a dramatic improvement in the precision of the $^{87}\text{Sr}/^{86}\text{Sr}$ ratio for each individual spot ablation. Note that similar improvement is not seen for $^{87}\text{Rb}/^{86}\text{Sr}$, as previously observed; the principal source of uncertainty on this ratio is derived from downhole fractionation of Rb/Sr during laser ablation. Overall, the improvements in precision of $^{87}\text{Sr}/^{86}\text{Sr}$ ratio results in Rb/Sr dates with roughly an order of magnitude higher precision (0.6%) compared to the 5% precision obtained via iCAP TQ ICP-MS (albeit with fewer ablation spots).

Bulk TIMS Rb-Sr analyses for the Dartmoor granite has previously yielded a whole rock isochron age of 284.6 ± 1.0 Ma (2σ)¹³. Our analysis of plagioclase and K-feldspar in DG-4 is accurate within uncertainty to the previously determined TIMS Rb/Sr age. Furthermore, the 0.6% precision of Rb/Sr age obtained from Neoma MS/MS ICP-MS is comparable with precision obtained via TIMS (0.3%).

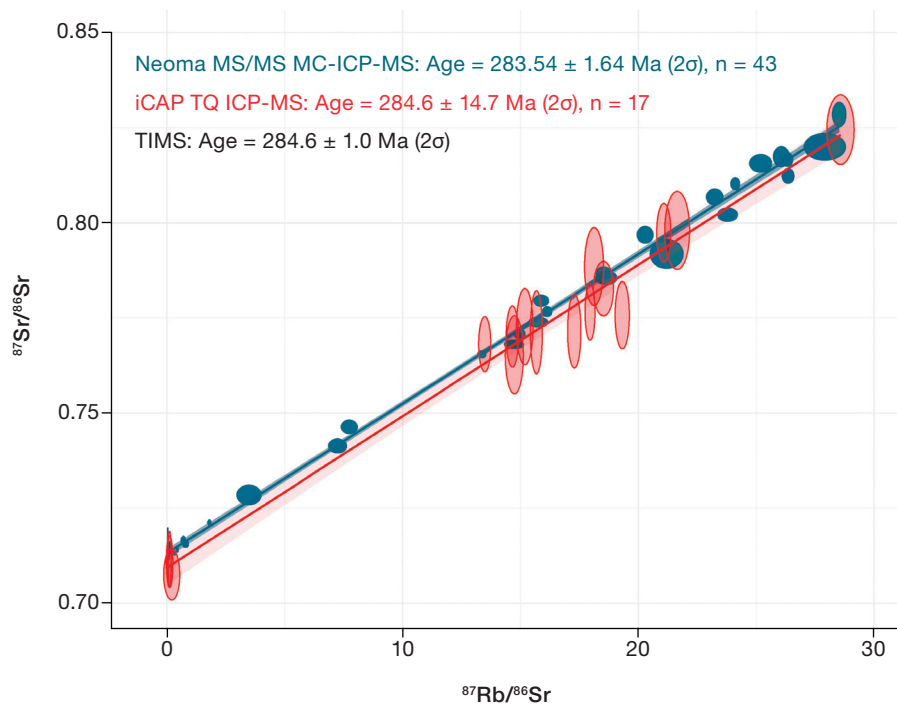


Figure 6. Rb/Sr isochron for Dartmoor Granite measured on Neoma MS/MS MC-ICP-MS (blue) and iCAP TQ ICP-MS¹¹ (red)

Micas in garnet-bearing schist

Unlike feldspar, micas (such as biotite and muscovite) have low mass fractions of strontium. Dating these samples using the Rb/Sr decay system may therefore seem more difficult as signal is limited, particularly on the minor Sr isotopes. Despite the higher noise of a Faraday detection system compared to an SEM, the higher sensitivity and multicollector array of the Neoma MS/MS MC-ICP-MS, using the Thermo Scientific™ $10^{13}\Omega$ Amplifier Technology™ is able to successfully determine Rb/Sr dates for low Sr biotite grains, Ra-D72.

A total of 19 ablation spots were used to determine the Rb/Sr date of the sample. Each analysis consisted of 20 s of background collection during laser warmup, 40 s of ablation, and 20 s of washout. A nanoparticle pressed powder pellet¹⁴ of phlogopite MicaMg was analyzed as a primary reference material. Each whole spot result is the average of 35 one second integrations.

Our analysis of 19 ablation spots of using the Neoma MS/MS MC-ICP-MS gives a calculated Rb/Sr date of 274.32 ± 10.8 Ma (2σ , Figure 7A), a great result for such a low Sr concentration sample. However, we observe that some of the spots have much larger error bars than others. These large error bars are not due to analytical uncertainty, but instead pointed to significant variability within the sample as the spot was ablated downwards. The static nature of the Neoma MS/MS MC-ICP-MS allows assessment of the sample heterogeneity. By looking at each individual 1 s integrations within a single spot, it is possible to generate an isochron for all 661 integrations contained within all 19 spot ablations (Figure 7B). In doing so we can see potentially a range of Rb/Sr dates within the sample.

Isochrons generated using just the 35 individual integrations from spot 5 (Figure 7C) reveal two distinct age zones within a single spot. The two dates have lower overall uncertainties on the isochron fits as the 19 whole spot ablations (Figure 7A), and also reveal age information of multiple events that are hidden by the conventional approach. There is huge potential for this type of single spot geochronology. Not only can it be used to assess sample heterogeneity through isotopic mapping, but it can be used to better characterize complex closure events within an individual crystal. By utilising the large collector array and high ohmic amplifiers of the Neoma MS/MS MC-ICP-MS, it is possible gain new information above and beyond the capabilities of traditional ICP-TQ-MS¹⁵.

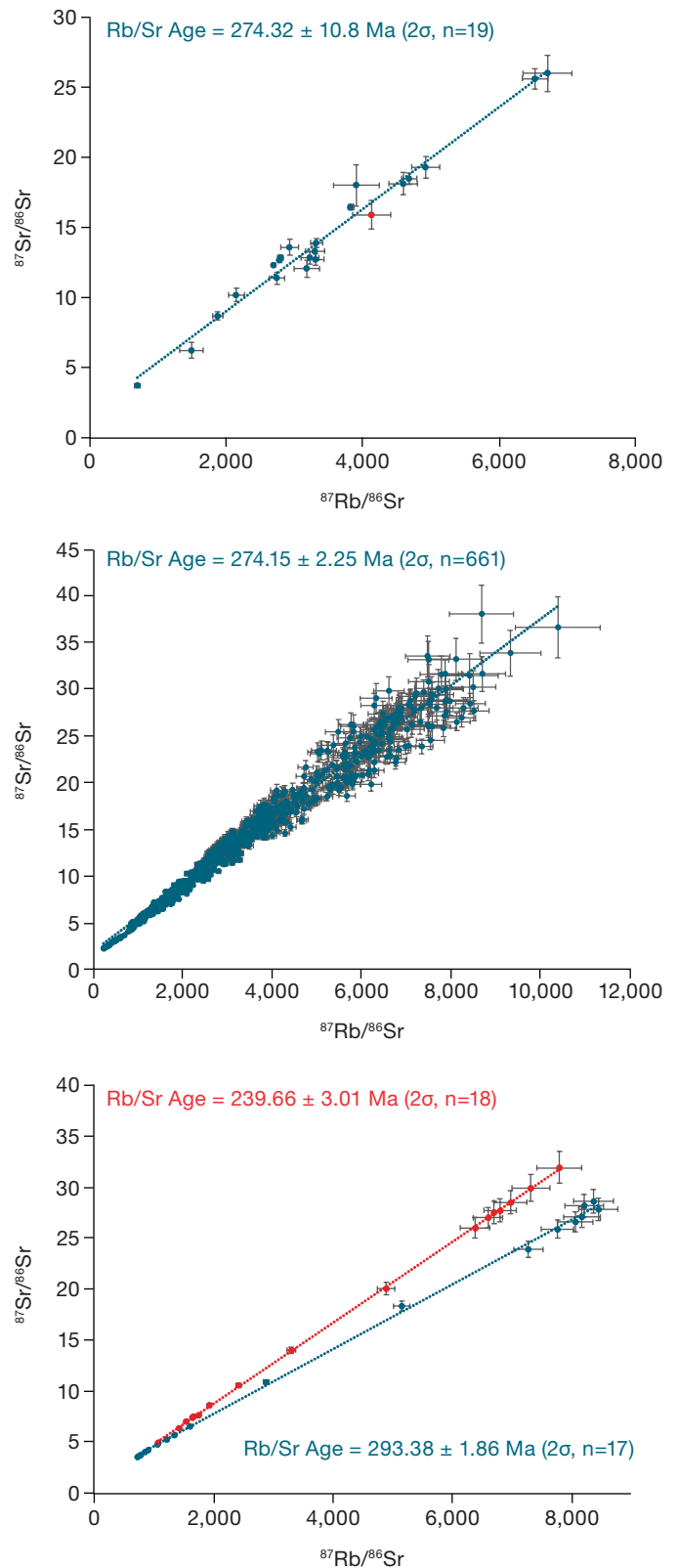


Figure 7. Rb/Sr isochrons for biotite from garnet-bearing schist sample (Ra-D72) measured on Neoma MS/MS MC-ICP-MS. (A) Whole spot analyses – Spot 5 highlighted in red (B) Individual Integrations (C) Single Spot Ablation – Spot 5.

Conclusion

Neoma MS/MS MC-ICP-MS is the first dedicated multicollector mass spectrometer with a collision cell and pre-cell mass filter. These technological innovations successfully separate Rb and Sr from matrix interferences, enabling for the first time static *in situ* Rb/Sr age dating. We have demonstrated here the implications of this fully static measurement for a range of geological targets.

For a series of reference glasses, we have demonstrated that Neoma MS/MS MC-ICP-MS can measure *in situ* $^{87}\text{Sr}/^{86}\text{Sr}$ ratios with a reproducibility of <1%. This precision is at the theoretical limit dictated by counting statistics and is an order of magnitude better than a dynamic peak hopping measurement using a single collector instrument.

We demonstrate how the improvement in the precision of the $^{87}\text{Sr}/^{86}\text{Sr}$ ratio affects the Rb/Sr ages measured in feldspar grains in granite. The precision of the Rb/Sr ages measured with Neoma MS/MS MC-ICP-MS are an order of magnitude better than the equivalent measurement made on a single collector instrument.

Finally, we showed the capability of the Neoma MS/MS MC-ICP-MS for static Rb/Sr measurement of muscovite grains with low Sr concentrations. The static nature of Neoma MS/MS MC-ICP-MS gives rise to a wealth of new information. We show how it is possible to generate multiple isochrons from a single ablation spot. Single spot dating has incredible potential, enabling assessment of intra-grain heterogeneity and even the creation of detailed Rb/Sr age maps of a single crystal.

References

1. Moens, L. J., Vanhaecke, F. F., Bandura, D. R., Baranov, V. I. & Tanner, S. D. Elimination of isobaric interferences in ICP-MS, using ion–molecule reaction chemistry: Rb/Sr age determination of magmatic rocks, a case study. *J Anal At Spectrom* 16, 991–994 (2001).
2. Tanner, S. D., Baranov, V. I. & Bandura, D. R. Reaction cells and collision cells for ICP-MS: a tutorial review. *Spectrochim Acta Part B At Spectrosc* 57, 1,361–1,452 (2002).
3. Vanhaecke, F., de Wannemacker, G., Moens, L. & van den Haute, P. The use of sector field ICP–mass spectrometry for Rb–Sr geochronological dating. *Fresenius' Journal of Analytical Chemistry* 2001 371:7 371, 915–920 (2001).
4. Tillberg, M., Drake, H., Zack, T., Hogmalm, J. & Åström, M. In Situ Rb–Sr Dating of Fine-grained Vein Mineralizations Using LA-ICP-MS. *Procedia Earth and Planetary Science* 17, 464–467 (2017).
5. Tillberg, M. et al. In situ Rb–Sr dating of slickenfibres in deep crystalline basement faults. *Scientific Reports* 2020 10:1 10, 1–13 (2020).
6. Hogmalm, K. J., Zack, T., Karlsson, A. K. O., Sjöqvist, A. S. L. & Garbe-Schönberg, D. In situ Rb–Sr and K–Ca dating by LA-ICP-MS/MS: an evaluation of N₂O and SF₆ as reaction gases. *J Anal At Spectrom* 32, 305–313 (2017).
7. Craig, G. et al. Project Vienna: A Novel PreCell Mass Filter for Collision/Reaction Cell MC-ICPMS/MS. *Anal Chem* 93, 10,519–10,527 (2021).
8. Dauphas, N. et al. In situ ^{87}Rb – ^{87}Sr analyses of terrestrial and extraterrestrial samples by LA-MC-ICP-MS/MS with double Wien filter and collision cell technologies. *J Anal At Spectrom* 37, 2,420–2,441 (2022).
9. Paton, C., Heilstrom, J., Paul, B., Woodhead, J., Hergt, J., Lolite: Freeware for the visualisation and processing of mass spectrometric data. *J Anal At Spectrom* 12, 2,508–2,518 (2011).
10. Rösel, D. & Zack, T. LA-ICP-MS/MS Single-Spot Rb–Sr Dating. *Geostand Geoanal Res* 46, 143–168 (2022).
11. Bevan, D. et al. In situ Rb–Sr dating by collision cell, multicollection inductively-coupled plasma mass-spectrometry with pre-cell mass-filter, (CC-MC-ICPMS/MS). *J Anal At Spectrom* 36, 917–931 (2021).
12. Wise, S. & Watters, R. Certificate of Analysis: Standard Reference Material 610. (2012).
13. Darbyshire, D.P.F. and Shepherd, T.J. *Journal of the Geological Society*, 142, 1,159–1,177 (1985).
14. Garbe-Schönberg, D. & Müller, S. *J Anal At Spectrom* 29, 990–1,000 (2014).
15. Cruz-Uribe, A.M., Craig, G., Garber, J.M., Paul, B., Arkula, C., Bouman, C., Single spot Rb–Sr isochron dating of biotite 1 by LA-MC-ICP-MS/MS, *Geostandards and Geoanalytical Research* (in press)

 Learn more at thermofisher.com/ms-ms

General Laboratory Equipment - Not For Diagnostic Procedures. © 2023 Thermo Fisher Scientific Inc. All rights reserved. All trademarks are the property of Thermo Fisher Scientific and its subsidiaries unless otherwise specified. Elemental Scientific Lasers and imageGEO193 are trademarks of Elemental Scientific Inc. NIST and SRM are registered trademarks of the National Institute of Science and Technology. This information is presented as an example of the capabilities of Thermo Fisher Scientific products. It is not intended to encourage use of these products in any manners that might infringe the intellectual property rights of others. Specifications, terms and pricing are subject to change. Not all products are available in all countries. Please consult your local sales representatives for details.
AN002246-EN 0623C